Pre-Conceptual Design of EU-Demo Divertor Primary Heat Transfer Systems

E. Vallone[a,*], L. Barucca[b], S. Ciattaglia[c], P.A. Di Maio[a], G. Federici[c], M. Giardina[a], I. Moscato[a], A. Quartararo[a], A. Tarallo[d]

[a]*Department of Engineering, University of Palermo, Viale delle Scienze, Ed. 6, 90128 Palermo, Italy*
[b]*Ansaldo Nucleare, Via N. Lorenzi 8, 16152 Genova, Italy*
[c]*EUROfusion Consortium, PPPT Department, Boltzmannstr. 2, Garching, Germany*
[d]*CREATE Consortium, Università di Napoli Federico II, Via Claudio 21, 80125 Napoli, Italy*

Abstract

In the frame of the activities promoted and encouraged by the EUROfusion Power Plant Physics and Technology (PPPT) department aimed at developing the EU-DEMO fusion reactor, strong emphasis has been recently addressed to the whole Balance of Plant (BoP) which represents the set of systems devoted to convert the plasma generated thermal power into electricity and to deliver it to the grid. Among these systems, the Divertor Primary Heat Transfer Systems (PHTSs) are intended to feed coolant to the two main components of the Divertor assembly, namely the Plasma Facing Components (PFCs) and the Cassette Body (CB). Since the DEMO Divertor must withstand high heat flux loads together with a considerable neutron deposited power, very tight tolerances may be allowed to the coolant inlet conditions. Therefore, the design of reliable PHTSs is of the utmost importance towards the development of an EU-DEMO fusion reactor. Within this framework, a study has been jointly carried out by University of Palermo, Ansaldo Nucleare and CREATE to design the Ex-Vessel PHTSs of both the PFCs and the CB for a DEMO reactor equipped with a Helium Cooled Pebble Bed Breeding Blanket. The paper describes criteria and rationale followed with the aim to achieve simple PHTS designs based on the adoption of easy-to-manufacture main components avoiding too much extrapolation from the state-of-art technology. Results of preliminary thermal-hydraulic calculations carried out to size heat exchangers, pressurizers, piping and pumps are presented and critically discussed, with particular attention to those integration, safety and feasibility constraints that may deeply affect the design of such components. Finally, the evaluation of PHTS key parameters as total pumping power and coolant inventory is reported.

Keywords: DEMO, Balance of Plant, PHTS, Divertor

1. Introduction

The European Research Roadmap to the Relisation of Fusion Energy has foreseen the production of electric power from nuclear fusion by the middle of this century [1]. In this framework, the EUROfusion consortium is developing the project of a DEMOnstration Fusion Reactor (DEMO) [2]. DEMO is going to be the first fusion device that will produce electricity and, hence, it should be Balance of Plant (BoP) "oriented" [3]. Furthermore, the DEMO BoP must meet many of those design criteria and safety requirements characterising the most common nuclear power stations [4].

In DEMO, BoP means the complex "chain" of systems devoted to the extraction of the pulsed thermal power generated by the plasma and its conversion into electric power to be delivered to the external grid, thus including both Ex-Vessel Primary Heat Transfer Systems (PHTSs) and Power Conversion System (PCS). Nevertheless, contrary to common Nuclear Power Plants (NPPs), DEMO is supposed to undergo a pulsed duty cycle during normal operating conditions. Consequently, it will be subjected to oscillating loads that might challenge the qualified lifetime of the main BoP equipment due to thermal and mechanical cycling. Although it is rather impossible to prevent the occurrence of such cycling in PHTS components, several strategies are being considered to mitigate the potential negative effects of the pulsed operations on PCS main

*Corresponding author
Email address: eugenio.vallone@unipa.it (E. Vallone)

components [5], such as turbine and steam generators.

In this direction, the leading approach followed for the BoP of a DEMO reactor equipped with a Helium Cooled Pebble Bed Breeding Blanket (HCPB BB) [6] is similar to that used in the solar energy industry. In order to thermally decouple the PCS from the BB PHTS, an Intermediate Heat Transfer System (IHTS) equipped with an Energy Storage System (ESS) is interposed among them (see fig. 1) [7]. This system acts as a bridge between the BB PHTS, which is the main hub of the DEMO heat transfer chain, and the PCS [8], allowing collecting a portion of the thermal power transferred during the Pulse period in order to save thermal energy to be delivered to the PCS during the Dwell time. The thermal power removed from Divertor (DIV) [9, 10] and Vacuum Vessel (VV) is used to pre-heat the PCS feed-water (see fig. 1), together with the most common regenerative heaters fed by the steam turbine extraction lines.

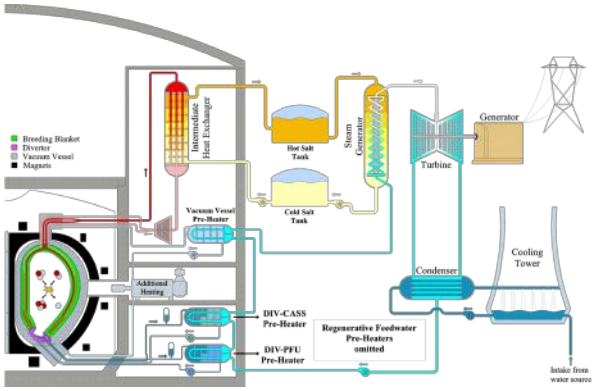

Figure 1: Simplified conceptual scheme of BoP - Indirect-coupling option.

In this context and within the framework of the activity of the Work Package Balance of Plant (WPBoP) of the EUROfusion actions, a study has been jointly carried out by University of Palermo, Ansaldo Nucleare and CREATE to design the main components of the Ex-Vessel PHTSs of the Divertor Plasma Facing Components (PFCs) and Cassette Body (CB), namely the DIVertor Plasma Facing Units (DIV PFU) PHTS and the DIVertor CASsette body (DIV CAS) PHTS, for a DEMO reactor equipped with a Helium Cooled Pebble Bed Breeding Blanket, assessing their sizes and the overall performances. The aim has been to identify technical R&D needs, establish layout integration and safety requirements [11].

The paper describes criteria and rationale followed with the aim to achieve simple PHTS designs based on the adoption of easy-to-manufacture main components avoiding too much extrapolation from the state-of-art technology. Results of preliminary thermal-hydraulic calculations carried out to size piping, heat exchangers and pressurizers are presented and critically discussed, with particular attention to those integration, safety and feasibility constraints that may deeply affect the design of such components. Finally, the evaluation of PHTS key parameters as total pumping power and coolant inventory is reported.

2. The design of the DIV PHTSs

According to DEMO Baseline 2017, the DEMO Divertor is articulated in 48 toroidal cassettes, three for each toroidal sector of the reactor, to ease their remote handling procedure. Each cassette is composed of a CB, equipped with a Shielding Liner and two Reflector Plates (RPs), and two PFCs, namely an Inner Vertical Target (IVT) and an Outer Vertical Target (OVT). IVT and OVT house the Plasma Facing Units (PFUs), the fundamental elements adopted to withstand the high superficial heat loads: they are cooling tubes, equipped with swirl tapes to enhance their heat transfer performances. Fig. 2 shows the CAD model of the entire Divertor assembly.

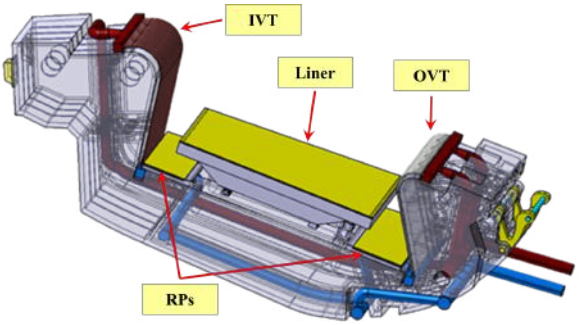

Figure 2: Model of the DEMO divertor assembly.

Due to the different heat loads they have to withstand and to the requirements agreed to guarantee the structural material integrity, the PFCs and the CB (with its Liner and RPs) must be cooled by two separate circuits, fed by water coolant at different thermal-hydraulic conditions.

The main function of the HCPB DIV PFU and DIV CAS PHTSs is to extract thermal power from Divertor PFCs and CB, respectively, and transfer it to the Power Conversion System through Heat eXchangers (HXs) that act as PCS feed-water pre-heaters as well as to provide containment boundary to the primary coolant. In

addition, they have also the function of limiting the air and secondary coolant in-leakage. The working pressure and temperature ranges are imposed by the operating conditions of the In-Vessel Components (IVC) cooling circuit, whose main thermal-hydraulic data may be found in [12, 13, 14] and in [15, 16, 17] for the PFCs and the CB, respectively. In particular, according to its pre-conceptual design, the DIV PFU PHTS is devoted to removing 136 MW of thermal power using water at a PFCs inlet pressure of 5 MPa and working temperatures of 130 ÷ 136 °C while the DIV CAS PHTS is devoted to removing 115.2 MW of thermal power using water at a CB inlet pressure of 3.5 MPa and working temperatures of 180 ÷ 210 °C.

Table 1 and table 2 summarize the main inputs and boundary conditions used to perform the detailed design of both the DIV PFU and DIV CAS PHTSs from the in-vessel client and the secondary side, respectively.

Table 1: Primary side input data and boundary condition.

	DIV PFU	**DIV CAS**
Coolant [-]	Water	Water
Divertor cassettes [-]	48	48
Deposited power [MW]	136.0	115.2
Inlet pressure [MPa]	5.00	3.50
Inlet temperature [°C]	130.0	180.0
Outlet temperature [°C]	136.0	210.0
Design pressure [MPa]	5.750	4.025
Design temperature [°C]	250.0	250.0
Pressure drop [bar]	9.436	8.452

Table 2: Secondary side input data and boundary condition.

	DIV PFU	**DIV CAS**
Coolant [-]	Water	Water
Inlet pressure [MPa]	0.40	5.90
Inlet temperature [°C]	62.7	165.6
Outlet temperature [°C]	112.6	201.7

The two PHTSs share the same layout; both the PHTSs are subdivided into two independent cooling loops, each one feeding eight Divertor sectors for a total of 24 Divertor cassettes. Each Divertor cooling loop is equipped with one pump, one pressurizer, one feed-water preheater and connecting piping. Loop interconnections have been avoided in order to reduce the maximum coolant inventory discharged following a pipe break in the Tokamak Cooling Rooms. The present layout is coherent with previous studies on fusion reactor balance of plant [18].

By way of example, the detailed design of the DIV PFU PHTS is reported in fig. 3 [19] with hot and cold zones of piping marked in red and blue colours, respectively. As can be recognized from the figures, the two loops are identical.

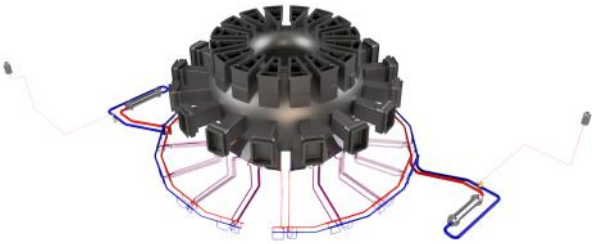

Figure 3: Isometric view of DIV PFU PHTS layout.

3. Pipework design and arrangement of the cooling loops

The main task of PHTS pipework is to transport the water coolant from the in-vessel components to the pre-heaters of the PCS feed-water and bring it back once the thermal power has been transferred to the PCS.

Concerning the pipe dimensions, nominal diameters have resulted from a compromise between the need of reducing the overall total pressure drop, and, thus, the pumping power, and the integration constraints. In particular, a coolant average velocity lower than 12 m/s should be kept within the largest pipework as a trade-off value between the need to limit system pressure drop (hence pumping power) and coolant total inventory. In particular, pipes nominal diameters range from DN125 to DN600 for the DIV PFU PHTS and from DN80 to DN300 for the DIV CAS PHTS.

Feeding pipes connecting either the Divertor PFCs or CB with the main distributors are equipped with several expansion bends to compensate for the large thermal expansion these types of cooling circuit may be subjected to during normal operations.

3.1. Pipe material and thermal insulation

The material preliminary selected for the pipe network of the DIV PHTSs is the stainless steel AISI 316LN (EN 1.4429, ASTM UNS S31653) mainly because it shows good high-temperature mechanical properties and its tritium permeation characteristics are well known [19].

Furthermore, the minimum insulation thicknesses required for the DIV PFU and DIV CAS feeding pipes to prevent excessive heat losses toward the environment have been calculated for the ex-vessel PHTS pipework up to the vacuum boundary of the upper port

annex (at Bio-shield level). Insulation material has been preliminary selected to be microporous insulation Microtherm® SLATTED [20] according to what has been done recently within the context of the ITER TBM programme [21] and to the available diameters from the Microtherm® catalogue. In particular, the calculated thicknesses range from 7 mm to 10 mm for the DIV PFU PHTS piping and from 14 mm to 20 mm for the DIV CAS PHTS piping.

3.2. Thermal-hydraulic design

In order to study the overall hydraulic behaviour of the system, an assessment of the pressure drops along the different paths of the DIV PFU and DIV CAS PHTS loops has been made. To this purpose, the evaluations have followed the approach usually suggested in the reference handbooks on this topic, such as the Idelchik's "Handbook of Hydraulic Resistance" [22] or "Pipe Flow" by Rennels and Hudson [23].

Concerning the pipework roughness, the value has been selected after a review of several sources [22, 23, 24], which report data that are not always in perfect agreement. Although it is clear that the roughness can have a non-negligible effect on the distributed pressure drops, especially in case of long piping systems as in the present case, it has been decided to apply in any case the value of 50 μm for conservative reasons. Furthermore, aiming at ensuring the required mass flow rate in each segment, a proper balance of the coolant pressure losses has been pursued assuming that dedicated zones of the loop will be equipped with devices suitable for this scope, such as tuning valves.

Fig. 6 and fig. 7 report a graphic representation of the pressure distribution along the central cassette cooling paths of the right half-ring, being representative of all the 24 cooling paths, for the DIV PFU PHTS and the DIV CAS PHTS, respectively. Furthermore, in order to ease the comprehension of fig. 6 and fig. 7, fig. 4 and fig. 5 illustrate the various "pressure-probing sections" for the cold and hot piping, respectively, of a typical DIV PHTS. The "tuning valves" are supposed to be placed along the cold feeding pipes before crossing the Bio-shield, i.e. between position 2 and 3.

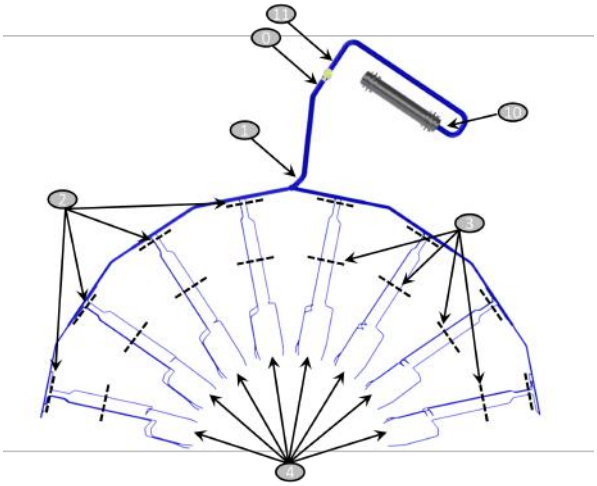

Figure 4: Cold piping pressure probing sections.

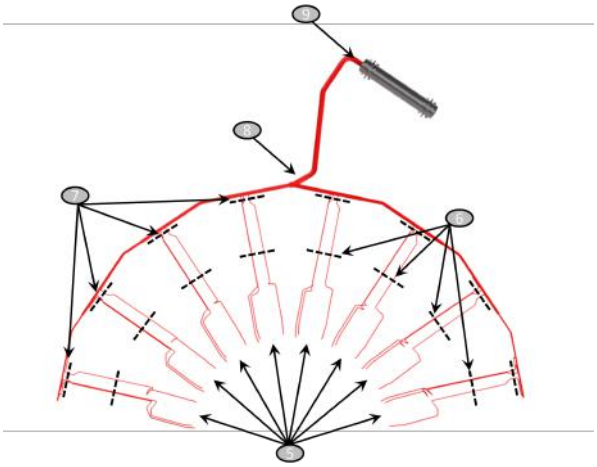

Figure 5: Hot piping pressure probing sections.

4. Heat exchanger design

Being the largest components of the ex-vessel circuits, the heat exchangers have been investigated as first priority because they can play an important role in the final disposition of the PHTS circuitry. If on the in-vessel component side the pipes must be channelled into the outer wall annexes to reach the lower pipe chase, on the exchangers side the arrangement of both hot and cold legs is driven by the heat exchanger topology, thus its inlet and outlet position strongly influence the overall PHTS layout.

In the nuclear industry, almost all the solutions adopt shell and tube heat exchangers; thus, the adoption of this typology appears the most logical choice if the application of proven manufacturing technologies wants to be pursued. Among the Shell&Tube (S&T) families, the "standard" configurations with straight or U-tube bundles are undoubtedly the most popular. Moreover, it is worth to underline that this kind of shell and tube heat exchangers is widely used also outside the nuclear industry; indeed, it is basically the "workhorse" of any

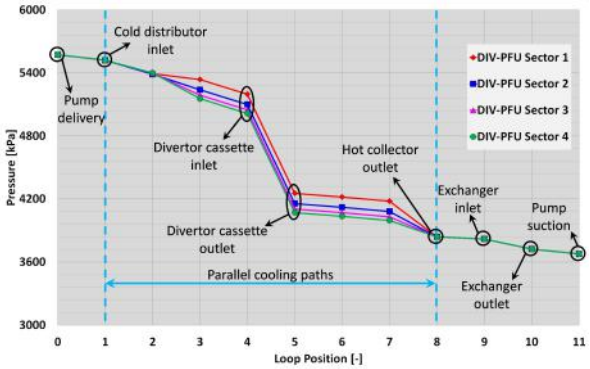

Figure 6: Static pressure distribution along the DIV PFU PHTS.

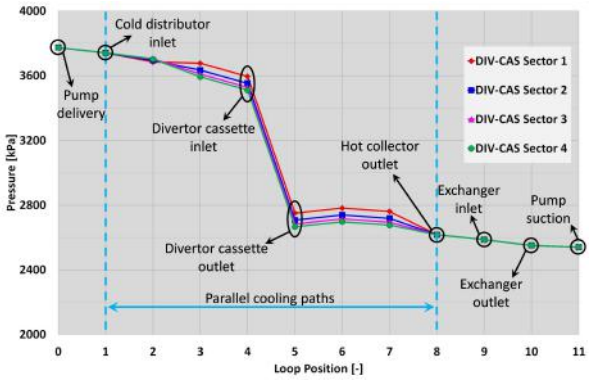

Figure 7: Static pressure distribution along the DIV CAS PHTS.

heat transfer industrial process for several reasons [25].

Therefore, first priority has been given to such an option because a positive assessment could exclude, or at least limit, the need of investigating heat exchangers more complicated to manufacture. The detailed description of the adopted design methodology is widely reported in [26].

Preliminary assessments have been made on both the two possible flow configurations of the shell fluid. In fact, keeping always an overall counter-current flow configuration between the primary and the secondary coolants, the fluid circulating on the shell side can ideally assume two main different flow patterns respect to the longitudinal axis of the bundle, namely pure parallel flow or pure cross flow.

Before starting with the first assessments, additional considerations and assumptions have been needed to circumscribe the boundaries within which to move and they will be introduced in the following. For instance, the selection of the tube-side fluid affects the choice of the exchanger typology and requires an evaluation of many factors to arrive at a satisfactory compromise.

For the DIV relevant fluids and working conditions, the choice of the tube-side coolant seems straightforward. Primary water coolant is the hottest fluid for both the DIV PFU and the DIV CAS and, flowing within a nuclear primary circuit, it is a carrier of radioactive particles (mainly tritium). Furthermore, a good prediction of its pressure losses is necessary to assess the pump size. Moreover, regarding the DIV PFU HX, primary coolant is the high-pressure fluid. Hence, the selection of the tube-side coolant is quite obligated in this case. The main input data and boundary condition can be gathered from table 1 and table 2.

4.1. Preliminary assessments and flow arrangement selection

A preliminary assessment has been carried out in order to narrow the field of possible options. A total of 1600 configurations have been investigated for each flow configuration considered, each one identified by a specific triad of independent variables: the tube external diameter "d_e" according to those available in the TEMA standard [27], the primary coolant maximum velocity "u_1" and the secondary coolant velocity "u_2". Their values ranging as follows:

- 15.875 mm $\leq d_e \leq$ 31.75 mm;
- 0.5 m/s $\leq u_1 \leq$ 7.5 m/s;
- 0.5 m/s $\leq u_2 \leq$ 1.5 m/s.

For a given triad of these values, the total number of tubes in the exchanger "N", the tube internal diameter "d_i", the shell side flow area "A_{cross}" (or ratio pitch over diameter "P/d_e") and, finally, the length of the tubes "L" can be calculated.

According to an engineering judgement, the cut-off points presently selected to consider feasible an option have been:

Max. tube length $L \leq 8$ m for the DIV PFU HX;

Max. tube length $L \leq 15$ m for the DIV CAS HX;

Max. internal shell diameter $D_i \leq 3$ m;

Max. tubes number $N \leq 5000$;

Pitch over diameter ratio $1.1 \leq P/d_e \leq 1.65$;

Max. primary side Δp $\Delta p_{Primary} \leq 2$ bar;

Max. secondary side Δp $\Delta p_{Secondary} \leq 1$ bar.

The geometrical constraints have been mainly selected in order to avoid too much extrapolation respect to the state-of-art technology limit. Additionally, as for the coolant pressure drop on both side of the exchanger, reasonable values drawn from the experience of fission NPPs have been considered.

Results have shown that, in case of parallel flow, just few options are feasible. On the contrary, if the HX is equipped with baffle plates, some more configurations are possible. Furthermore, for a given triad of tube diameter, primary and secondary coolant speed, the plate-baffled shell and tube exchanger allows to minimize the heat transfer surface; therefore, it has been chosen to focus the attention on this option to be studied in detail. Some of the most relevant results obtained for the DIV PFU are shown in figures from fig. 8 to fig. 11. The values in black represents points that lie outside the design constraints.

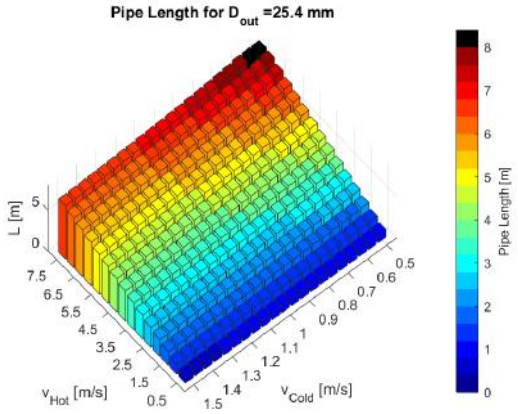

Figure 8: Tube length for d_e = 25.4 mm.

4.2. Detailed design

The analysis of the preliminary results has led to select the plate-baffled shell and tube exchanger. In addition, a wide variety of primary and secondary coolant velocity combination may be selected. In order to definitely select the tubes diameter, a check of the nominal dimensions commonly available on the market has been done. The need of thousands tubes to equip two heat exchangers per PHTS suggests the use of standard sizes, unless particular conditions would occur.

The tube minimum thickness has been calculated by the proper formula drawn from ASME code [28]:

$$t_{min} = \frac{p_{design} d_e}{2(S_m + p_{design} Y)} + A \quad (1)$$

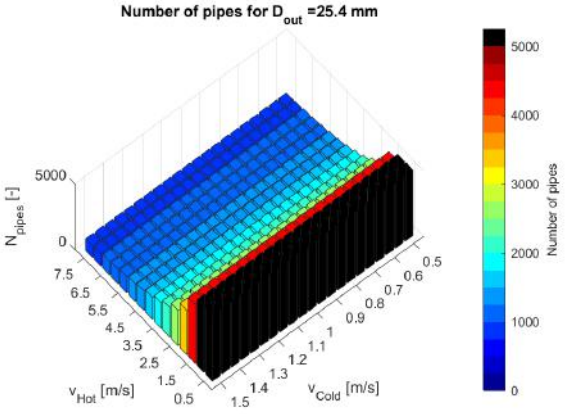

Figure 9: Number of tubes for d_e = 25.4 mm.

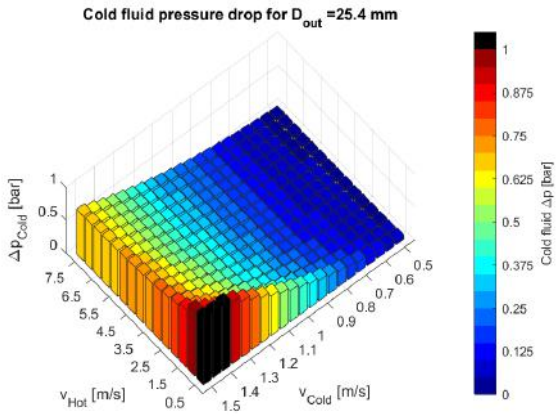

Figure 10: Secondary side pressure drop for d_e = 25.4 mm.

where p_{design} is reported in table 1, Y is equal to 0.4 and S_m is the maximum allowable stress intensity of the tube material at the design temperature, set to 250 °C for both the DIV PHTSs. This latter value takes into account the temperature that the PHTS is supposed to reach in case it undergoes the baking operative procedure [10]. The A factor is an allowance that can be added to the minimum calculated value to consider any reason that could lead to a reduction of the material (e.g. corrosion, erosion, wall thinning do to treatments). An allowance of 0.1 mm has been employed.

Therefore, performing the calculations it has been seen that to lay within the optimal internal diameter region, a nominal d_e = 25.4 mm with a wall thickness of 1.245 mm must be used for the DIV PFU HX while a nominal d_e = 15.875 mm with a wall thickness of 1.651 mm must be adopted for the DIV CAS HX. The final thicknesses have been selected so to avoid the possible

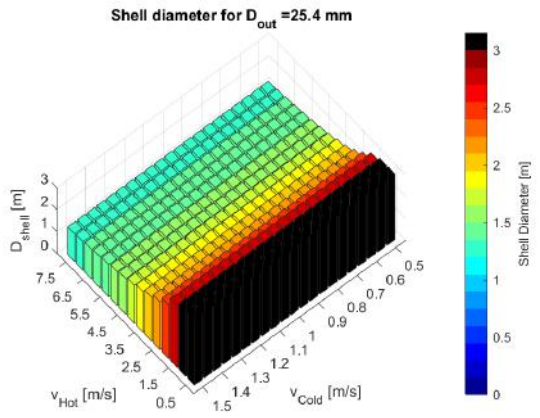

Figure 11: Shell diameter for d_e = 25.4 mm.

occurrence of tube buckling due to the different thermal expansion between the tube and the shell material during operations. As regard to the tube layout and the pitch, a square tube lattice with a pitch of 38.1 mm has been selected.

To ensure proper heat transfer capabilities also in the so-called "End-of-Life" (EoL) conditions, a 10% oversizing of the exchanger is usually envisaged. Furthermore, in the EoL conditions, the fouling factor on the secondary side has been set to $1.76{\cdot}10^{-4}$ m^2K/W according to [27], while no fouling factor has been used for the primary coolant, being confident in its high cleanliness during operation.

After a proper tube allocation within the shell has been pursued taking into account the presence of supporting tie rods, the internal shell diameter has been selected together with dimensions and distribution of the shell internal baffle for both the DIV HXs, considering reasonable clearances [26]. Moreover, the employment of an annular distributor at the inlet nozzle has been foreseen to slow down the entering coolant thus avoiding vibrations and erosion of the first rows of the tube bundle.

Once these main geometrical characteristics have been set, the detailed thermal-hydraulic design of the plate-baffled heat exchangers has been performed following the Bell-Delaware approach, as modified by Taborek [29]. The Bell-Delaware method is based on the calculation of a series of auxiliary geometrical factors for the determination of the shell side heat transfer coefficients and pressure drops. These factors are all listed in many handbooks that deal with this topic [29, 30].

Furthermore, a preliminary mechanical assessment of the principal pressure retaining elements of both the exchangers has been made. In particular, the thicknesses of the shell parts and the plates have been evaluated by means of the rules and the guidelines reported in the different sections of ASME Boiler and Pressure Vessel Code (BPVC), namely section III [28, 31] and section VIII [32].

Therefore, in agreement with all the criteria and constraints described, a final design for both the standard shell and tube DIV HXs has been outlined. By way of example, the DIV PFU exchanger layout and the coolant flow scheme are reported in fig. 12. The main thermal-hydraulic characteristics resulted from the assessments are summarized in table 3 while the main outcomes of the mechanical design are reported in table 4.

It must be pointed out that the calculations have been run in parallel with those for pipework and pumps (see section 3 and section 6) allowing assessing, through an iterative procedure, the inlet pressure of the exchanger as well as its outlet temperature.

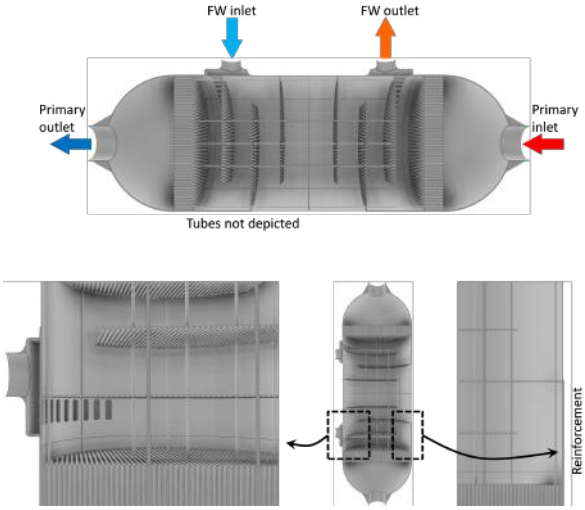

Figure 12: Preliminary sketch of the DIV PFU HX.

Primary water coolant enters into the "hot" hemispherical head, here it is canalized into the tube bundle through the holes drilled in the tubesheet. Feedwater flows on the shell side where it enters through 18 openings connecting the heating section to an annular distributor (pre-chamber) in which the water is injected from the inlet nozzle. The annular distributor is necessary to slow down the coolant thus avoiding vibrations and erosion of the first rows of the tube bundle. In the heating section, primary and secondary coolants have an overall counter current flow pattern, with the feed-water crossing the baffle compartments. At the outlet of the tube bundle, after being passed through the tubesheet,

Table 3: Main thermal-hydraulic features of the DIV HXs.

	DIV PFU	**DIV CAS**
Inlet pressure Tube/Shell side [MPa]	3.82/0.4	2.59/5.95
Inlet temperature Tube/Shell side [°C]	136.0/62.7	210.0/165.5
Outlet temperature Tube/Shell side [°C]	129.6/112.6	179.7/201.7
Mass flow rate Tube/Shell side [kg/s]	2728.5/360.1	431.4/367.8
Number of tubes BOL[-]	2633	4525
Number of tubes EOL [-]	2369	4072
Fouling factor BOL Tube/Shell side [m^2K/W]	0/0	0/0
Fouling factor EOL Tube/Shell side [m^2K/W]	0/1.76E-4	0/1.76E-4
Heat transfer surface BOL [m^2]	834.5	2969.6
Heat transfer surface EOL [m^2]	750.8	2672.3
Tube external diameter [mm]	25.4	15.875
Tube pitch [mm]	38.1	23.813
Tube lattice [-]	square	square
Tube thickness [mm]	1.245	1.651
Tube active length [m]	3.972	13.159
Tube material [-]	Inconel 690	Inconel 690
Primary Volume [m^3]	10.6	11.6
Secondary Volume [m^3]	12.3	26.6
Primary mass [t]	9.9	10.1
Secondary mass [t]	11.9	23.6
Mean overall heat transfer coefficient [W/m^2K]	2427	1988
Primary side pressure drop [kPa]	95.7	36.1
Secondary side pressure drop [kPa]	56.8	202.2

Table 4: Additional mechanical data of the DIV HXs.

	DIV PFU	**DIV CAS**
Shell material [-]	SA-508 Gr.3 Class 2	SA-508 Gr.3 Class 2
Tubesheet material [-]	SA-508 Gr.3 Class 2	SA-508 Gr.3 Class 2
Tube material [-]	Inconel 690	Inconel 690
Overall height [mm]	6968.0	15907.0
Shell external diameter (no discontinuities zones) [mm]	2322.0	1966.0
Shell external diameter (reinforced zones) [mm]	2346.0	1998.0
Shell thickness (no discontinuities zones) [mm]	8.0	32.0
Shell thickness (reinforced zones) [mm]	20.0	48.0
Head external diameter [m]	2346.0	1998.0
Head thickness [mm]	20.0	48.0
Tubesheets thickness [mm]	325	375
Reinforcement length (at tubesheet discontinuity) [mm]	1000	1000
Baffle spacing [mm]	496.5	657.95
Baffle thickness [mm]	12.7	19.1
Tube-to-baffle hole clearance (diametral) [mm]	0.4	0.4
Shell-to-baffle clearance (diametral) [mm]	10.8	9
Shell-to-bundle clearance (diametral) [mm]	65	65
Total metal mass [ton]	32	80

the primary fluid is collected into the "cold" head from which it exits and is carried to the pump suction via a cold leg. The secondary coolant exits the shell through an annular collector where the outlet pipe nozzle is attached. The exchanger will be placed in horizontal position.

5. Preliminary pressurizer sizing

Since the DIV PHTSs are cooled by highly subcooled water and no boiling is allowed to ensure that the IVC may safely operate under normal operative conditions, each PHTS loop must be equipped with a pressurizer (PRZ), which acts as a surge volume.

Due to the peculiar pressure and temperature operating ranges of the DIV PHTSs, the common design approach [33, 34] adopted for a typical PWR might have led to the underestimation of the pressurizer liquid and vapour volumes needed to accommodate any out-surge or in-surge transient. Therefore, it has been further developed considering plausible overcooling and overheating scenarios with pragmatic margins according to the methodology adopted for the ITER IBED PHTS pressurizer [35].

Furthermore, the minimum pressurizer diameter to avoid liquid swelling to the pressurizer relief valve with a reasonable safety margin has been calculated for both the DIV PHTS PRZs, according to [36].

Moreover, a preliminary mechanical sizing has been carried out for both the two PRZs following the indications given in [37] and the maximum stresses at the head joints are evaluated according to [38].

In this context, it is worth to underline that a proper pressurizer sizing shall take into account a profound knowledge of the thermal-hydraulic behaviour of the investigated PHTS under the most relevant operational and incidental transient scenarios. Therefore, the results herein presented are to be intended as preliminary component sizing rather than a final pressurizer design.

5.1. Pressurizer volumes allocation

According to the methodology outlined in [35], enough space for the following five points must be considered while allocating pressurizer volume. The final pressurizer dimension is simply given by the sum of the five allocated volumes.

1. Nominal and transient surge space.
2. Steam space for spray nozzle/steam condensation.
3. Heater length in cylinder.
4. Level measurement uncertainty.
5. Operating margin at extent of measurement range.

These points allow taking into account the necessary volumes to accommodate the expansion and contraction of the coolant in order to maintain pressure control during plasma operations and transient events.

The primary loop is schematized as consisting of two sections, namely a Hot Section (HS) and a Cold Section (CS). Coolant thermo-physical properties in the hot and cold legs are conservatively based on the thermal-hydraulic conditions calculated at the heat exchanger entrance and at the pump delivery section, respectively. In-vessel components and HX volumes have been equally divided between hot and cold sections. Furthermore, coolant pressure within the pressurizer has been assumed close to that calculated at the heat exchanger entrance ($\approx$38.2 bar for the DIV PFU PHTS and $\approx$25.9 bar for the DIV CAS PHTS), i.e. where the surge line is supposed to be connected to the hot leg. Initially, the system is uniformly supposed at the cold leg temperature in a so-called "hot stand-by" state (T = 130 °C for the DIV PFU PHTS and T = 180 °C for the DIV CAS PHTS).

The pressurizer volume is excluded from this calculation because it does not experience the changes in temperature that the rest of the system does. The main input parameters are reported in table 5.

Table 5: Pressurizer sizing input parameters.

	DIV PFU	**DIV CAS**
In-vessel volume [m^3]	3.841	35.209
HX volume [m^3]	10.585	11.602
HS piping volume [m^3]	18.056	7.662
CS piping volume [m^3]	23.576	7.217
Nominal HS volume [m^3]	25.269	31.068
Nominal CS volume [m^3]	30.789	30.623
HS pressure [bar]	38.2	25.9
Nominal HS temperature [°C]	136.0	210.0
CS pressure [bar]	55.7	37.7
Nominal CS temperature [°C]	130.0	180.0
Pressurizer pressure [bar]	37.2	24.9
Pressurizer temperature [°C]	246.1	223.8

5.2. Pressurizer diameter estimation

The procedure described in [35] and adopted for the DIV PHTS PRZs allows calculating the total volume of the pressurizers, while nothing is still known about its cross-section area and, thus, on its height-to-diameter ratio. In common NPPs, this latter value typically amounts to $4 \div 5$, it strongly depends on the adopted venting equipment and on the pressure control system and it is derived from the investigation of some relevant

transient scenarios according to the criteria established by the licensing authority.

At the pre-conceptual phase, transient simulations have not been performed for the DIV PHTSs neither during operational scenarios nor during incidental ones. Rather, a preliminary sizing is needed to start an iterative design that might also take into account the outcomes of relevant transient analysis. To this purpose, aiming at determining a tentative reasonable value for the pressurizer diameter, some interesting observations on vapour disengagement dynamics can be made.

Depressurization of a vessel containing superheated liquid or addition of heat to liquid in a vessel gives rise to the formation of vapour bubbles, which results in liquid swell. If this is severe, the level of the swollen liquid may reach the vent. Even if this is not so, there may be carryover of droplets into the vent. Liquid swell and vapour disengagement therefore affect the vapour mass fraction entering the vent [39].

In the following, the methodology outlined in [36] is exploited to get a tentative reasonable value for the pressurizer diameter.

The models described herein are applicable to top-vented, vertical, right circular cylindrical vessels when it has been established that two-phase flow will occur and that some vapour-liquid disengagement will take place.

In order to ensure that the pressurizer might safely operate under normal and off-normal conditions, the occurrence of liquid swelling to the relief valve and, thus, of a two-phase venting must be prevented. If it is conservatively assumed an all vapour vent mass flow rate, the vapour material balance at the vent entrance may be written as:

$$A_v G = j'_{g\infty} \rho_{g,s} A_{CR} \tag{2}$$

where A_v is the vent cross-section area, G is the vent mass flux, $j'_{g\infty}$ is the vapour superficial velocity at the liquid surface which is required to just swell the liquid to the top of the vessel (the subscript ∞ refers to the value at the liquid surface), $\rho_{g,s}$ is the vapour density at the vessel super-incumbent pressure and temperature, A_{CR} is the vessel cross-section area.

The vapour superficial velocity ($j'_{g\infty}$) can be calculated from an appropriate vessel model that relates $j'_{g\infty}$ to the vessel average void fraction ($\bar{\alpha}$). Vessel flow models estimate the liquid swell (degree of vapour-liquid disengagement) as a function of vapour throughput. These vessel flow models are then coupled with vent flow capacity models at a given vessel pressure to determine the vapour mass fraction and the total mass flow rate entering the vent line which in turn allows determination of the vent volumetric discharge rate [36]. The vessel flow models define the relationship between the average void fraction in the swelled liquid ($\bar{\alpha}$), the vapour superficial velocity at the liquid surface ($j'_{g\infty}$), and the characteristic bubble rise velocity (U_∞).

Two principal regimes are recognized as occurring when a vessel is depressurized. If the liquid is non-foaming the regime tends to be churn-turbulent, whereas if it is foaming the regime is bubbly [39]. An otherwise non-foaming liquid may be rendered foaming by the presence of impurities. The water coolant of a primary heat transfer system of a nuclear power plant may undoubtedly be classified as a non-foaming fluid. Therefore, the churn-turbulent vessel model has been deemed the most suitable to describe the pressurizer of the DIV PHTSs.

The churn-turbulent vessel model assumes uniform vapour generation throughout the liquid with considerable vapour-liquid disengagement in the vessel. The degree of vapour-liquid disengagement is represented by the relationship:

$$\frac{j'_{g\infty}}{U_\infty} = \frac{2\bar{\alpha}}{1 - C_0\bar{\alpha}} \tag{3}$$

where C_0 is a data correlating parameter with normal values running from 1.0 to 1.5. According to [36], C_0 = 1.0 is conservative while C_0 = 1.5 may be considered a best-estimate value. The first value has been deemed too conservative; therefore, C_0 = 1.5 has been adopted for the present calculation. The characteristic bubble rise velocity (U_∞) for the churn-turbulent vessel model is given by the expression:

$$U_\infty = 1.53 \frac{[\sigma g(\rho_f - \rho_g)]^{1/4}}{\rho_f^{1/2}} \tag{4}$$

where σ is the interfacial tension, g is the acceleration due to gravity, ρ_f is the liquid density, and ρ_g is the vapour density. $\bar{\alpha}$ can be set equal to the vessel average void fraction to estimate the maximum vapour superficial velocity for the onset of two-phase venting for given values of U_∞ and C_0.

Given the needed theoretical background, the following procedure is proposed to obtain a tentative pressurizer diameter.

Step 1. The average void fraction within the pressurizer (α_{PRZ}) is calculated from the volumes allocated in the previous section simply as:

$$\alpha_{PRZ} = \frac{V_g}{V_g + V_f} \tag{5}$$

where V_g is the pressurizer volume occupied by the steam during normal operation while V_f is the space occupied by the saturated liquid. At this stage, a safety factor (K) may be applied so to have a minimum safety margin from liquid swelling at least during normal operation. Accounting for this safety margin, the average void fraction in the swelled liquid ($\bar{\alpha}$) is set to:

$$\bar{\alpha} = K\alpha_{PRZ} \tag{6}$$

where K has been assumed equal to 0.9 for the present calculation.

Step 2. Given $\bar{\alpha}$, the degree of vapour-liquid disengagement ($j'_{g\infty}/U_\infty$) may be evaluated from eq. (3) according to the churn-turbulent vessel model.

Step 3. U_∞ is calculated from eq. (4) for the churn-turbulent vessel model and, thus, $j'_{g\infty}$.

Step 4. If the valve throat area and the valve mass flux are known or may be somehow assumed, eq. (2) may be conveniently rearranged to give the minimum pressurizer cross-section area:

$$A_{CR} = \frac{A_v G}{j'_{g\infty}\rho_{g,s}} \tag{7}$$

The last step of the outlined sizing procedure requires that the valve throat area and the valve mass flux are somehow known. These values are usually evaluated by means of transient simulations that allow calculating the maximum mass flow rate to be evacuated during reference incidental scenarios. Nevertheless, as transient calculations are not yet available, the valve throat area may be tentatively assumed by scaling those drawn from common NPPs.

Following some simple considerations, the valve throat area may be considered as proportional to the reactor power and inversely proportional to the volume of the PHTS and the valve set point. Therefore, the valve throat area ($A_{v,i}$) can be scaled from [40] by means of the following equation:

$$A_{v,i} = A_{v,PWR}\frac{Q_i}{Q_{PWR}}\frac{p_{PWR}}{p_i}\frac{V_{PWR}}{V_i} \tag{8}$$

where $A_{v,PWR}$, Q_{PWR}, p_{PWR} and V_{PWR} are drawn from [40] and are representative values of, respectively, valve throat area, reactor thermal power, valve set point and PHTS volume for fission NPPs. On the other hand, Q_i, p_i and V_i are, respectively, reactor thermal power, valve set point and PHTS volume of either a DIV PFU or a DIV CAS PHTS loop.

While sizing the Safety Relief Valve (SRV), it must be considered that the usual requirement for a SRV is to keep the maximum pressure drop in the PHTS pipework during any transient scenario below $1.1p_{design}$ (see [40]). Therefore, taking into account the predicted total pressure drop between the pump delivery and the surge line connection, the SRV pressure set points have been fixed to ≈44.8 bar for the DIV PFU PHTS and ≈31.5 bar for the DIV CAS PHTS. Additionally, following the EPR example [40], the pressurizer is supposed to be equipped with three SRV mounted on top of it while Power Operated Relief Valves (PORVs) are not considered.

Concerning the mass flux through the valve, it may be calculated according to [28] and presuming that an all-vapour vent flow occurs by means of the following equation:

$$G = \frac{5.25C_d(1.1p_{SRV} + p_{atm})10^6}{3600} \tag{9}$$

where G is the mass flux through the valve expressed in $\mathrm{kgs^{-1}m^{-2}}$, C_d is the discharge coefficient, p_{SRV} and p_{atm} are respectively the SRV set pressure gauge and the atmospheric pressure both expressed in MPa. C_d is calculated following the indications given in [28] and amounts to 0.873.

The pressurizer cross-section area may now be calculated from eq. (7). Table 6 reports the main outcomes of the pressurizer sizing.

Table 6: Pressurizer sizing summary.

	DIV PFU	**DIV CAS**
Cylinder volume [m^3]	9.170	5.777
Single head volume [m^3]	0.714	1.432
Total volume [m^3]	10.597	8.642
Liquid volume [m^3]	5.346	4.879
Vapour volume [m^3]	5.251	3.763
Diameter [m]	1.760	2.220
Cylinder height [m]	3.769	1.493
Total height [m]	4.649	2.603
Height to diameter ratio [-]	2.14	0.67
PRZ cross-section area [m^2]	2.433	3.871
PRZ operating pressure [bar]	37.2	24.9
Number of SRV [-]	3	3
SRV pressure set point [bar]	44.8	31.5
SRV throat area [m^2]	$2.317{\cdot}10^{-3}$	$2.641{\cdot}10^{-3}$

5.3. Preliminary mechanical design

The thicknesses of the pressurizer shell parts have been preliminarily evaluated by means of the rules and the guidelines reported in [37]. Furthermore, the maximum axial and hoop stresses at the head joints are evaluated according to [38].

The low alloy steel SA-533 Type B CL1 has been preliminary selected for the pressurizer and its properties have been drawn from [41].

Table 7: Pressurizer preliminary mechanical design summary.

	DIV PFU	DIV CAS
Shell material [-]	SA-533 Type B CL1	
Design stress intensity [MPa]	184.0	
Design pressure [MPa]	5.75	4.025
Shell selected thickness [mm]	34.0	28.0
PRZ external diameter [m]	1.818	2.246
PRZ external height [m]	4.759	2.684
PRZ metal weight [ton]	7.409	4.569
Max. axial stress [MPa]	160.7	171.2
Max. hoop stress [MPa]	166.9	177.8

6. Preliminary considerations on pump selection

The PHTS Main Coolant Pumps (MCPs) must provide forced-circulation flow to the IVC sufficient to ensure that they might safely operate during normal and off-normal condition preventing the occurrence of the departure from nucleate boiling with a sufficient safety margin. To this purpose, the MCPs shall be sized to deliver the IVC flow rate with adequate margin. Table 8 reports the MCPs main design parameters for both the DIV PFU and DIV CAS PHTSs.

Table 8: MCPs main design parameters.

	DIV PFU	DIV CAS
Rated vol. flow rate [m^3/s]	2.912	0.486
Rated head [m]	206	142
Isentropic efficiency [-]	0.80	0.80
El./mech. efficiency [-]	0.95	0.95
Thermal power [MW]	6.89	0.749
Electrical power [MW]	7.26	0.789

With regard to table 8, the rated head has been calculated from the results summarised in section 3 while typical isentropic and electrical/mechanical efficiencies have been assumed for the calculation of the thermal power deposited into the fluid and the required electrical power.

With reference to the most modern fission NPPs, it may be argued that almost all of them are equipped with vertical shaft, single stage, single suction, centrifugal primary pumps.

In particular, it may be noticed that primary pumps of common PWRs are usually characterised by high rated capacities and relatively low heads if compared to what expected for the DIV PHTSs. Motor speed varies in a short range comprised between 900 and 1200 rpm, while the required electric power ranges between 4.5 and 7.5 MW.

Instead, when looking at the Boiling Water Reactors (BWRs) and CANDU technology, the rated volumetric flow rates and the developed heads are much closer to those predicted for the DIV PFU PHTS, but still far from what is expected for the DIV CAS PHTS. The electric power is in the same range already identified for the PWRs, while the nominal speed is typically higher (1800 rpm).

On the other hand, auxiliary systems of common NPPs, such as the component cooling water system and the residual heat removal system [42], are typically equipped with centrifugal pumps whose operating parameters are close to those expected for the DIV CAS PHTS.

Therefore, in line with the nuclear industry experience, it seems quite natural that the quest for a pump design solution shall be oriented towards a vertical, single stage, centrifugal pump within a nominal speed ranging between 800 and 1800 rpm and employing a controlled leakage shaft-seal assembly.

7. Integration of the DIV PHTSs in the DEMO Tokamak Building

From the previous sections, it can be summarized that a generic DIV PHTS loop consists of in-vessel circuits, an heat exchanger, a pressurizer, a main coolant pump and connecting pipes.

The piping (per each cooling loop) foresees hot leg, cold leg, collector, distributor and six feeding pipes per each sector (3 pipes to retrieve hot water from each sector and 3 to feed them with cold water). Feeding pipes connecting the DIV-PFUs to the main manifolds are routed within the lower ports through radial penetrations across the Bio-shield. Coolant manifolds are hosted in a toroidal corridor, the so-called Lower Pipe Chase (LPC), running all around the Tokamak. Hot (cold) manifolds of each circuit are arranged in order to form a hot (cold) half-ring, which collects (distributes) the coolant among the feeding pipes. Half-rings have variable cross section to minimize the coolant inventory and keep the water velocity below 12 m/s. Hot legs and cold legs respectively connect the manifolds to the HXs and the MCPs to the distributors. The main cold and hot legs cross the LPC outer wall to reach HXs and MCPs rooms. Piping is equipped with a proper thermal insulation.

The main components are located on the two opposite sides in the Tokamak cooling rooms at the lower levels

of the Tokamak Building. The HXs are integrated in the BoP Rankine cycle as pre-heaters of the feed-water. The feed-water flows on the secondary side. Each HX relies on the Shell&Tube technology.

The pressurizers are connected to the hot legs upstream the heat exchangers through surge lines. They maintain the systems pressure at operating conditions and compensate for changes in coolant volumes due to load variations.

The MCPs are located nearby the exit of the HXs; a crossover pipe connects the HX to MCP, which, downstream, is connected to the cold leg. The MCPs are required to deliver and maintain an appropriate flow through the primary system according to the loading conditions during: DEMO power operation (e.g. Pulse, Dwell phases), start-up and shut-down operations, operational residual heat removal (e.g. hot/cold stand-by).

Table 9 provides a brief summary of the data characterizing the DIV primary systems. By way of example, the global arrangement of the DIV PFU PHTS is reported in fig. 13 while its integration into the Tokamak building is shown fig. 14.

Table 9: Main DIV PHTSs architecture design parameters.

	DIV PFU	DIV CAS
Number of cooling loops [-]	2	2
Pump electrical power [MW]	14.5	1.6
In-vessel water volume [m^3]	7.7	70.4
Ex-vessel water volume [m^3]	106.7	59.8
Water volume [m^3]	114.4	130.2
Pipework length [m]	2545.0	2787.0

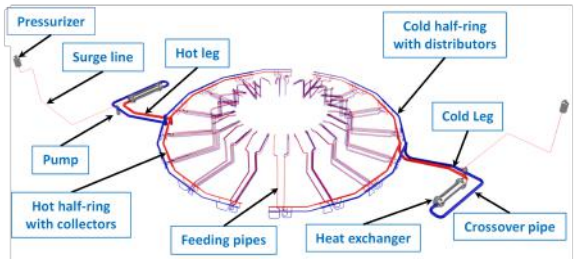

Figure 13: Overview of the HCPB DIV PFU PHTS.

8. Conclusions

Within the framework of the pre-conceptual design activity of the WPBoP of the EUROfusion PPPT Department, the DIV primary systems have been sized considering a two-loop segmentation option. These circuits are completely independent, from a mechanical point of view, also in order to limit some common failures mode.

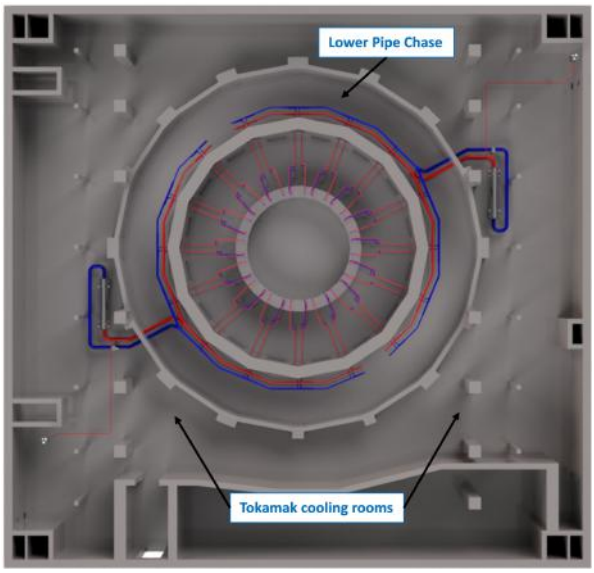

Figure 14: Integration of the DIV PFU PHTS into the Tokamak building (top view).

A preliminary design of the main relevant components of the systems such as HXs, PRZs and connection pipes has been performed following good engineering practices and according to trade-off analysis to find the best compromise solution among the available options.

Further step will address the review of the DIV PHTS design in light of the update of the requirement coming from the IVC clients [43, 44].

CRediT authorship contribution statement

E. Vallone: Conceptualization, Methodology, Investigation, Writing - original draft. **L. Barucca**: Conceptualization, Methodology, Investigation, Writing - original draft. **S. Ciattaglia**: Conceptualization, Methodology, Investigation, Writing - original draft. **P.A. Di Maio**: Conceptualization, Methodology, Investigation, Writing - original draft. **G. Federici**: Conceptualization, Methodology, Investigation, Writing - original draft. **M. Giardina**: Conceptualization, Methodology, Investigation, Writing - original draft. **I. Moscato**: Conceptualization, Methodology, Investigation, Writing - original draft. **A. Quartararo**: Conceptualization, Methodology, Investigation, Writing - original draft. **A. Tarallo**: Conceptualization, Methodology, Investigation, Writing - original draft.

Declaration of Competing Interest

The authors declare that they have no known competing financial interests or personal relationships that could have appeared to influence the work reported in this paper.

Acknowledgments

This work has been carried out within the framework of the EUROfusion Consortium and has received funding from the Euratom research and training programme 2014-2018 and 2019-2020 under grant agreement No 633053. The views and opinions expressed herein do not necessarily reflect those of the European Commission.

References

[1] T. Donné, W. Morris, European Research Roadmap to the Realisation of Fusion Energy, 2018, ISBN: 978-3-00-061152-0.

[2] G. Federici, et al., Overview of the DEMO staged design approach in Europe, Nuclear Fusion 59 (2019) 066013. doi:10.1088/1741-4326/ab1178.

[3] L. Barucca, et al., Status of EU DEMO heat transport and power conversion systems, Fusion Engineering and Design 136 (2018) 1557–1566. doi:10.1016/j.fusengdes.2018.05.057.

[4] S. Ciattaglia, et al., EU DEMO safety and balance of plant design and operating requirements. Issues and possible solutions, Fusion Engineering and Design 146 (2019) 2184–2188. doi:10.1016/j.fusengdes.2019.03.149.

[5] L. Barucca, et al., Pre-conceptual design of EU DEMO balance of plant systems: objectives and challenges, this conference.

[6] F.A. Hernández, et al., Consolidated design of the HCPB Breeding Blanket for the pre-Conceptual Design Phase of the EU DEMO and harmonization with the ITER HCPB TBM program, Fusion Engineering and Design 157 (2020) 111614. doi:10.1016/j.fusengdes.2020.111614.

[7] I. Moscato, et al., Progress in the design development of EU DEMO helium-cooled pebble bed primary heat transfer system, Fusion Engineering and Design 146 (2019) 2416–2420. doi:10.1016/j.fusengdes.2019.04.006.

[8] E. Bubelis, et al., Industry supported improved design of DEMO BoP for HCPB BB concept with energy storage system, Fusion Engineering and Design 146 (2019) 2334–2337. doi:10.1016/j.fusengdes.2019.03.183.

[9] J.H.You, et al., Progress in the initial design activities for the European DEMO divertor: Subproject "Cassette", Fusion Engineering and Design 124 (2017) 364–370. doi:10.1016/j.fusengdes.2017.03.018.

[10] G. Mazzone, et al., Eurofusion-DEMO Divertor - Cassette Design and Integration, Fusion Engineering and Design 157 (2020) 111656. doi:10.1016/j.fusengdes.2020.111656.

[11] C. Gliss, et al., Initial layout of DEMO buildings and configuration of the main plant systems, Fusion Engineering and Design 136 (2018) 534–539. doi:10.1016/j.fusengdes.2018.02.101.

[12] P.A. Di Maio, et al., Hydraulic analysis of EU-DEMO divertor plasma facing components cooling circuit under nominal operating scenarios, Fusion Engineering and Design 146 (2019) 1764–1768. doi:10.1016/j.fusengdes.2019.03.030.

[13] P.A. Di Maio, et al., On the thermal-hydraulic optimization of DEMO divertor plasma facing components cooling circuit, Fusion Engineering and Design 136 (B) (2018) 1438–1443. doi:10.1016/j.fusengdes.2018.05.032.

[14] P.A. Di Maio, et al., Thermal-hydraulic behaviour of the DEMO divertor plasma facing components cooling circuit, Fusion Engineering and Design 124 (2017) 415–419. doi:10.1016/j.fusengdes.2017.02.025.

[15] P.A. Di Maio, et al., Thermal-hydraulic optimisation of the DEMO divertor cassette body cooling circuit equipped with a liner, Fusion Engineering and Design 146 (2019) 220–223. doi:10.1016/j.fusengdes.2018.12.024.

[16] P.A. Di Maio, et al., Computational thermofluid-dynamic analysis of DEMO divertor cassette body cooling circuit, Fusion Engineering and Design 136 (B) (2018) 1588–1592. doi:10.1016/j.fusengdes.2018.05.063.

[17] P.A. Di Maio, et al., Analysis of steady state thermal-hydraulic behaviour of the DEMO divertor cassette body cooling circuit, Fusion Engineering and Design 124 (2017) 437–441. doi:10.1016/j.fusengdes.2017.02.012.

[18] A. Natalizio, J. Collén, Final Report on SEAFP Task M8 COOLING SYSTEM DESIGN PART A: WATER COOLANT OPTION, 1994, SEAFP/R-M8/F(94).

[19] A. Tarallo, et al., Preliminary CAD implementation of EU-DEMO primary heat transfer systems for HCPB breeding blanket option, Fusion Engineering and Design 146 (2019) 2062–2065. doi:10.1016/j.fusengdes.2019.03.102.

[20] MICROTHERM® SLATTED, https://www.promat.com/en/industry/technologies/microporous/microtherm-slatted/3905/.

[21] L. Giancarli, et al., Overview of recent ITER TBM Program activities, Fusion Engineering and Design 158 (2020) 111674. doi:10.1016/j.fusengdes.2020.111674.

[22] I.E. Idelchik, Handbook of Hydraulic Resistance, Jaico Publishing House, 2008.

[23] D.C. Rennels, H.M. Hudson, Pipe Flow - A practical and Comprehensive Guide, Wiley, 2012.

[24] K. Siemens, Conceptual design of the Cooling System for A DEMO Fusion Reactor with Helium Cooled Solid Breeder Blanket, 1992, KfK contract No. 315/03179710/0102.

[25] T. Kuppan, Heat Exchanger Design Handbook, CRC Press Taylor & Francis Group, 2013.

[26] I. Moscato, Thermal-hydraulic study in support of the design of the DEMO Balance of Plant, Ph.D. thesis, Department of Engineering, University of Palermo, Handle: http://hdl.handle.net/10447/395492 (2020).

[27] TEMA, Standards of the Tubular Exchanger Manufacturers Association, Tubular Exchanger Manufacturers Association, Inc., 2007.

[28] ASME, ASME BPVC - Section III - Division 1 - Subsection NB, ASME, 2015.

[29] E.U. Schlunder, Handbook of Heat Exchager Design, Hemisphere Publishing, 1983.

[30] S. Kakaç, et al., Heat Exchangers -Selection, Rating, and Thermal Design, CRC Press, 2012.

[31] ASME, ASME BPVC - Section III - Division 5 - High Temperature Reactors, ASME, 2015.

[32] ASME, ASME BPVC - Section VIII - Division 1, ASME, 2015.

[33] N.E. Todreas, M.S. Kazimi, Nuclear Systems, Vol. 1, Thermal Hydraulic Fundamentals, CRC Press, 2012.

[34] NRC, NRC Issuances: Opinion and Decisions, Vol. 13, Section E, Pressurizer and Quench Tank sizing.

[35] J. Berry, TCWS IBED PHTS Pressurizer Sizing Calculation, ITER_D_94USPN v2.0.

[36] Harold G. Fisher, Emergency Relief System Design Using

DIERS Technology, Chapter 1: Vapor Disengagement Dynamics, American Institute of Chemical Engineers, 1992.
[37] ASME, ASME BPVC - Section III - Division 1 - Subsection NC, ASME, 2015.
[38] Ansel C. Ugural, Stresses in Beams, Plates, and Shells, CRC Press, 2010.
[39] S. Mannan, Lee's Loss Prevention in the Process Industries, Hazard Identification, Assessment and Control, Vol. 1, Elsevier, 2005.
[40] I. AREVA NP, U.S. EPR FINAL SAFETY ANALYSIS REPORT, Tier 2, Revision 5, Chapter 5, Section 5.4.
[41] ASME, ASME BPVC - Section II - Subsection D, ASME, 2015.
[42] I.J. Karassik, J.P. Messina, P. Cooper, C.C. Heald, PUMP HANDBOOK, McGraw-Hill, 2008.
[43] P.A. Di Maio, et al., On the numerical assessment of the thermal-hydraulic operating map of the DEMO Divertor Plasma Facing Components cooling circuit, Fusion Engineering and Design 161 (2020) 111919. doi:10.1016/j.fusengdes.2020.111919.
[44] P.A. Di Maio, et al., On the thermal-hydraulic performances of the DEMO divertor cassette body cooling circuit equipped with a liner, Fusion Engineering and Design 156 (2020) 111613. doi:10.1016/j.fusengdes.2020.111613.